ISSN 1064-2269, Journal of Communications Technology and Electronics, 2019, Vol. 64, No. 6, pp. 581–589. © Pleiades Publishing, Inc., 2019.
Russian Text © The Author(s), 2019, published in Radiotekhnika i Elektronika, 2019, Vol. 64, No. 6, pp. 575–584.

THEORY AND METHODS OF SIGNAL PROCESSING

Radar Interferometric Survey of the Surface of an Unprepared Landing Area from on Board a Helicopter

A. I. Baskakov[a], O. V. Chernoyarov[a, b, c, *], A. A. Komarov[a], and M. S. Mikhailov[a]

[a] *National Research University MEI, Moscow, 111250 Russia*

[b] *International Laboratory of Random Process Statistics and Quantitative Financial Analysis, Tomsk State University, Tomsk, 634050 Russia*

[c] *Maikop State Technological University, Maikop, 385000 Russia*

**e-mail: chernoyarovov@mpei.ru*

Received January 29, 2018; revised January 29, 2018; accepted February 2, 2018

Abstract—The paper considers the possibilities of radar interferometric survey of the surface of a landing site from on board a helicopter. It is shown that if the phase-difference dependence obtained in this way is superimposed on the radio-brightness pattern of the reflection according to resolution elements after irradiation of the studied surface under study, then it is possible to reconstruct a high-quality three-dimensional image of the landing area and to determine with high accuracy its possible slope, the characteristics of its relief, and the contours of foreign objects on it.

DOI: 10.1134/S1064226919060019

INTRODUCTION

One of the main causes of helicopter accidents is unreliable tools for landing on an unprepared landing area (LA) in adverse weather conditions in the day and at night with poor visual visibility conditions. Even in the case of good weather, dusty or snowy ground during landing can endanger the lives of the pilot and crew. The massive dust or snow cloud formed by swirling air due to helicopter's rotors can substantially mask the LA. As well, irregularities with heights of 0.5 m or more and inclinations of the LA greater than 15° already are dangerous for helicopter landings, especially in strong winds. Most helicopters are equipped with satellite navigation systems and airborne radio altimeters, which provide the pilot with precise and accurate positioning while flying and descending, but do not provide necessary information on the state of the LA relief and possible foreign objects on it. There are also modern methods for synthesizing multichannel adaptive processing algorithms using antenna arrays for detecting and resolving signals in conditions of a priori parametric uncertainty [1, 2]. This paper proposes a different approach: it is shown that, for known antenna system characteristics and irradiation geometry, the task of processing signals reflected from foreign objects on the LA and from surface relief elements can be effectively solved with a radar interferometric algorithm, which can visualize the LA surface.

1. FORMULATION OF THE PROBLEM

In recent years, radar interferometric methods have been used for real-time high-precision mapping of large areas of the underlying surface, since the functionality and information content of onboard remote radio-sensing tools significantly increase with reception of three-dimensional terrain images in a wide swatch and the required resolution. The interferometric method involves obtaining information about the elevations of the relief in each resolution element via measurement of the phase difference of the reflected signals at the inputs of two offset antenna systems [3, 4]. In this case, there are three possible variants of interferometric survey:

(1) with a "soft" base, which assumes suveying of the same surface area with monostatic radar on two or more consecutive flyovers with a certain time interval;

(2) with a "hard" base, in which the distance between the antennas is fixed on one carrier, with one of the antennas performing emission and reception, and the other, recpetion only;

(3) with a variable base formed from monostatic radars on different carriers located on synchronously connected flight paths.

For real-time receipt of necessary information about the state of the LA relief and possible foreign objects on it, interferometric survey with a hard base is most suitable.

A radar survey of the surface of the LA to ensure helicopter safety during landing at a speed of no more

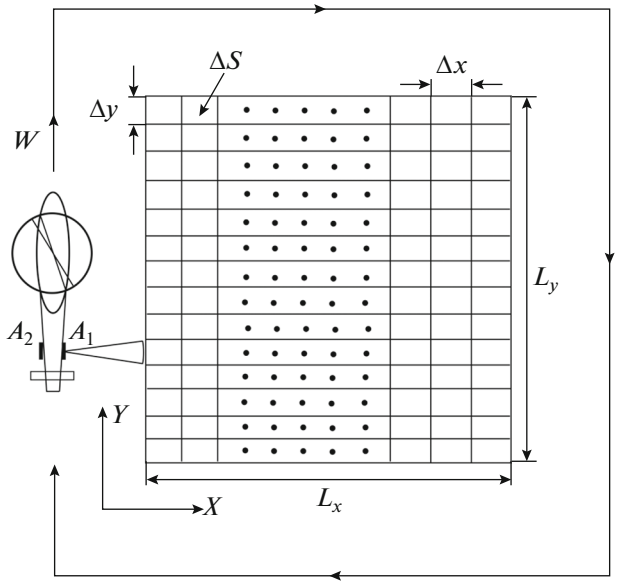

Fig. 1. Flight path of helicopter when viewing landing site: L_x, L_y, dimensions of LA along x and y axes; Δx, Δy, range and azimuth resolution, respectively; ΔS, area of resolution element.

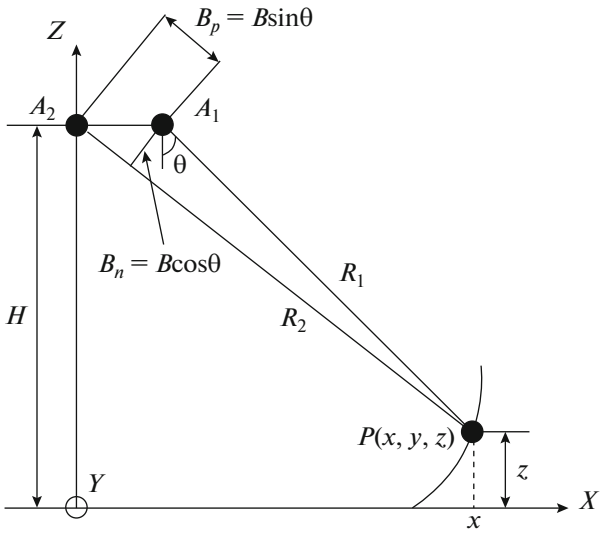

Fig. 2. Geometry of irradiation for calculating parameters of probe signal.

than 15 m/s should be carried out from a height of $H = 50–100$ m. At the beginning of the survey, the helicopter's coordinates are specified by a satellite navigation system. According to flight regulations [5], the size of the LA should be be at least two diameters of the helicopter rotors, about 90 × 90 m. At the same time, before landing on an unprepared LA, the helicopter must perform a maneuver the trajectory of which corresponds to overflight of the selected LA, as shown in Fig. 1. The choice of the operating frequency of the system in the Ka-band is governed by minimization of the antennas sizes and the necessary high resolution of the onboard radar, as well as the effect of radio-wave transmission losses.

The radar antenna system consists of two antennas directed at the same area of the of LA surface: transceiver $A1$ and receiver $A2$, implemented as slotted waveguide arrays connected by a hard base with size B mounted in parallel on the helicopter's tail boom and moving along the y axis at velocity W (Fig. 2). The coordinates of the phase centers of antennas $A1$ and $A2$ of the onboard radar with horizontal orientation of the base correspond to values of (x_1, y_0, z_1) and (x_2, y_0, z_1), and the coordinates of the current surface irradiation element P, (x, y, z). The ratio of the linear length of the antenna l_a and the length of the radio wave λ makes it possible to form a narrow beam in the azimuthal plane Δy. The beam widths of antennas $A1$ and $A2$ in the elevation plane are identical and cover a range of angles determined by the size of the LA at the selected flight altitude H.

The high range discrimination is

$$\Delta x = c/(2\Delta f \sin\theta)$$

ensured by a probe signal with nanosecond resolution. Here c is the speed of light, Δf is the spectral width of the probing signal, $\theta = \arccos(H/R_1)$ (R_1 is the distance of the transceiver antenna $A1$ to the area of the irradiated surface). The azimuth resolution Δy is determined by the antenna siz, since for the selected helicopter flight altitudes and size of the LA under specific flight conditions, radar operation in the azimuthal plane occurs in the near field of the antennas.

2. PECULIARITIES IN ESTIMATING BACKSCATTERING FROM THE EARTH'S SURFACE

When developing a theoretical model of backscattering by the Earth's surface in the Ka-band, four types of open surfaces were considered: (1) a wet plowed field with large lumps of soil, (2) dry sand, (3) a concrete runway, and (4) a wet asphalt road with 0.5 mm of rainwater. Table 1 shows the rms roughness ordinate s, correlation length, and relative dielectric constant ε_r of these surfaces.

We denote by σ^0 the specific effective scattering surface (ESS). Using the semiempirical model described in [6, 7] for three types of polarization—horizontal (HH), vertical (VV), and cross-polarization (HV), we represent the backscattering of radio waves from the above surfaces as follows:

$$\sigma^0_{VV} = g\frac{\cos^b\theta}{\sqrt{p}}[\Gamma_{VV}(\theta) + \Gamma_{HH}(\theta)],$$
$$\sigma^0_{HH} = p\sigma^0_{VV}, \quad \sigma^0_{HV} = q\sigma^0_{VV}. \tag{1}$$

Table 1. Surface parameters

Surface type	s, mm	l, mm	ε_r	Ref.
Wet plowed field	7.77	20	$5.9 + j3.5$	[6, 7]
Dry sand	2.62	30	$3.1 + j0.3$	[7, 8]
Concrete strip	0.34	4.2	$2.5 + j0.65$	[5, 8]
Wet asphalt with rainwater	0.34	0.5	$7.4 + j4.8$	[9]

Here θ is the angle of incidence, Γ_{VV} and Γ_{HH} are the Fresnel reflection coefficients for the corresponding polarization, $\Gamma_0 = \left|\left(1-\sqrt{\varepsilon_r}\right)\Big/\left(1+\sqrt{\varepsilon_r}\right)\right|^2$ is the coefficient of reflection to the nadir, $g = 2.2[1-\exp(-0.2ks)]$, $b = 3.5 + (1/\pi) \times \arctan[10(1.64-ks)]$, $p = \left[1-(2\theta/\pi)^{1/3\Gamma_0}\right] \times \exp(-0.4ks)]^2$, $q = 0.23\sqrt{\Gamma_0} \times [1-\exp(-0.5ks\sin\theta)]$, $k = 2\pi/\lambda$ is the wavenumber.

According to [10], the estimate for the background signal intensity from the LA surface is calculated taking into account losses in the antenna-feeder path and in the worst weather conditions, i.e., in the rain. The background/noise ratio is determined by the basic radar equation:

$$q = 10\log\left[\frac{PG^2\lambda^2}{(4\pi)^3 R^4 N_0 \Delta F}\right] + \sigma_{\Delta S} - \gamma - \eta, \qquad (2)$$

where P is the transmitter power, G is the antenna gain, R is range of action N_0 is the spectral density of the noise power at the receiver input, ΔF is the receiver band, $\sigma_{\Delta S} = \sigma^0_{pp}\Delta S$ is the ESS of the surface of the LA resolution element, σ^0_{pp} is specific ESS surface (1) for the corresponding polarization pp (VV, HH, or HV), γ are radio-wave losses in rain or a dusty or snowy environment, and η are losses in the antenna-feeder path.

The field of large-scale surface irregularities of the LA is reconstructed under the assumption of a linear three-scale model of the reflecting surface. According to this model, the height of irregularities at each point of the observed surface area is the linear superposition of three spatiotemporal fields: the field of small irregularities comparable to the length of the transmitted radio wave and forming a diffuse-scattered signal, the field of large irregularities significantly exceeding λ and imparting to the reflected signal additional amplitude-phase modulation, and the mesoscale relief field that determines the average inclination of the underlying surface. It is assumed that the characteristics of the mesoscale relief are constant in the zone of the LA surface. We consider the fields of small and large irregularities mutually independent uniform random fields in the spatiotemporal domain of observation.

Reflections from an elementary resolvable area ΔS_n form a single reading of the received signal corresponding to the nth range interval. We assume that Δz is unknown height of the resolved area, which consists of large-scale irregularities and increments of the mesoscale relief measured from the plane $z_0 = 0$. It should be noted that as a result of backscattering from the Earth's surface, a background is created, which significantly affects the characteristics of detection of foreign objects on the LA. Under these conditions, foreign objects should be detected taking into account the signal/(background + noise) ratio.

In recent publications by Russian authors [11–14, etc.], new efficient algorithms have been developed to automate detection of stationary and slowly moving man-made objects based on (1) the contrast of their ESS to reflections from the Earth's surface and (2) polarization features. The energetic signal/(background + noise) ratios are found during implementation of the search procedure for man-made objects on the helicopter's LA, which ensure acceptable operational quality of these detection algorithms in practice. Below, is a method is considered that can significantly increase the visualization of man-made objects on the LA when phase-difference information on the reflected signals arriving at the two antennas is used. It is shown that since dangerous irregularities in the LA relief, such as hills and ravines, should be detected taking into account the background/noise ratio, the phase-difference information makes it possible to detect large irregularities of the relief in radar images with determination of their relative height.

3. ALGORITHM FOR ONBOARD RADAR INTERFEROMETRIC SURVEY OF THE SURFACE OF A LANDING AREA

After the necessary processing, radar signals emitted by the first antenna and received by the two receivers form an interferogram [15]. Algorithm for calculating height z the resolution element of the phase difference of signals arriving at two antennas from the same resolution element, from the geometry of sight, is determined by the following expression (see Fig. 2):

$$z = H - R_1\left\{\cos\alpha\sqrt{1-\left[\frac{R_1^2 + B^2 - (R_1 - \Phi/k)^2}{2BR_1}\right]^2} + \sin\alpha\left[\frac{R_1^2 + B^2 - (R_1 - \Phi/k)^2}{2BR_1}\right]\right\}, \qquad (3)$$

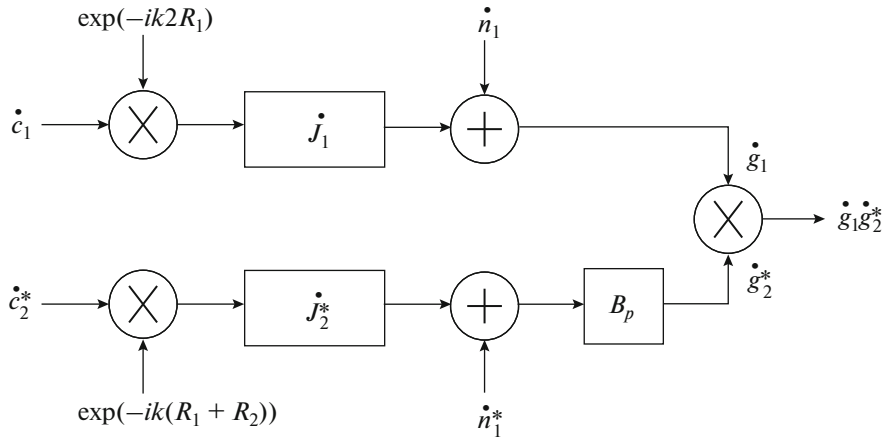

Fig. 3. Model of radar interferometric survey.

where R_1 is the slant range, H is the helicopter flight altitude, α is the base tilt angle relative to the horizon, in this case zero, B is the antenna base of the interferometer, $\Phi = (2\pi/\lambda) B \sin\theta$ is he phase difference, and k is the wavenumber.

The total error in measuring the roughness height z of a resolution element caused by the following: variance in the estimate of the height of the resolution element is $\sigma^2_{z\Phi}$ due to the error in estimating the phase difference, the error in adjusting the base angle $\sigma^2_{z\alpha}$, the error in measuring the helicopter flight altitude σ^2_{zH}, the error in measuring the distance to the resolution element $\sigma^2_{zR_1}$, and the error of inaccurate knowledge of the size of the base σ^2_{zB}. When determining the helicopter flight altitude, the mean-square error of the height estimate H can be reduced to several centimeters with modern radio altimeters and the values of other components are determined by the design features of the antenna system and the stability in piloting the helicopter. The the accuracy in measuring the roughness height z is impacted the most significantly by the error in measuring the phase difference of the interferometer signals.

An radar-survey interferogram is formed in a radar by multiplication of one image by a complex-conjugate second image of the same subject, but obtained from a different antenna. Figure 3 shows a model of a radar interferometric survey using two complex images, where exp (·) is the phase shift due to the propagation of radio waves, $\dot{J}_{1,2}$ *is the* impulse response of the path, n is thermal noise, $\dot{g}_{1,2}$ is the radar's complex output signal, B_p is the delay for compensation of the signal delay at the base.

To analyze the phase difference, the maximum likelihood method is used. Then, the estimate for the phase difference from each resolution element on the surface is written as [16]

$$\hat{\Phi} = \arctan\left[\mathrm{Im}\left(\sum_{n=1}^{N} \dot{g}_{1n} g^*_{2n}\right) \Big/ \mathrm{Re}\left(\sum_{n=1}^{N} \dot{g}_{1n} g^*_{2n}\right)\right], \quad (4)$$

where N is the multiplicity of incoherent accumulation.

The error in estimating the phase difference σ_Φ that occurs in the processing of echo signals can be written as

$$\sigma_\Phi = \sqrt{\left(\hat{\Phi} - \langle\hat{\Phi}\rangle\right)^2} = \frac{1}{\sqrt{2N}} \frac{\sqrt{1-\gamma_q^2}}{\gamma_q}, \quad (5)$$

where

$$\gamma_q = f(\Omega_\eta) M_\chi(\Omega_\chi) / (1 + 1/q) \quad (6)$$

is the correlation of the echo signals coming to two antennas [16, 17];

$$f(\Omega_\eta) = \exp\left[-\left(B\cos\theta / k_1 \lambda R \tan\theta\right)^2 \left(c/2\Delta f\right)^2\right]$$

is the "base-decorrelation" function, which characterizes the decorrelation of signals due to the offset of the two antennas and change in dimensions of the resolution element on the surface;

$$M_\chi(\Omega_\chi) = \exp\left[-2\pi^2 \left(\sigma_\chi B \cos(\alpha - \theta)/\lambda H \tan\theta\right)^2\right]$$

is the characteristic function of small surface irregularities within the resolution element, which determines the degree of signal decorrelation due to the presence of small roughness with root-mean-square ordinate σ_χ on the large relief of the LA, k_1 is the approximation constant, which is determined from the ratio $(\sin x/x)^2 \approx \exp\left[-(k_1 x)^2\right]$, q is the signal/noise ratio.

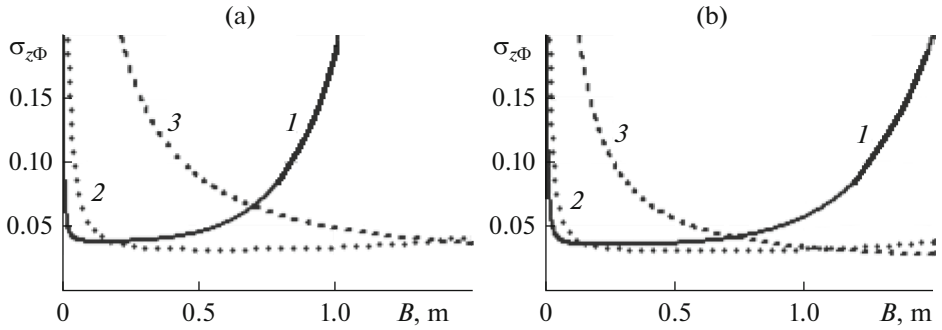

Fig. 4. Dependence of fluctuation error in measuring resolution element ordinates $\sigma_{z\Phi}$ on size of antenna base B for $\sigma_\chi = 7.8$ (a) and 2.62 mm (b) and various viewing angles: $\theta = 30$ (*1*), 45 (*2*) and 60° (*3*).

For such an irradiation geometry, the fluctuation error in measuring the z coordinate of the resolution element $\sigma_{z\Phi}$ is determined by the ratio [17]

$$\sigma_{z\Phi} = \frac{\lambda H \tan\theta}{2\pi B \cos(\alpha - \theta)}\sigma_\Phi. \quad (7)$$

Studies show that there is an optimal antenna base B of a radio interferometer, which is selected based on the minimum error in measuring the z ordinate. For example, let us set the following values: helicopter flight altitude $H = 75$ m, radio wavelength $\lambda = 8.6$ mm, multiplicity of incoherent accumulation with each resolution element $N = 16$. The beam patterns in the elevation plane are identical and cover the dimensions determined by the LA in the angle range 30°–60°, which gives a slant range from $R_{\min} = 85$ m to $R_{\max} = 150$ m at the chosen flight altitude.

Figure 4 shows the calculated potential accuracy of the method: the dependence of the fluctuation error in measuring the height of a resolution element $\sigma_{z\Phi}$ on the size of the antenna base B at $\theta = 30°$, 45° and 60° and two values of σ_χ [17, 18]. It can be seen that for a small antenna base, the sensitivity of the system to the relief is weak and for large B values, signals arriving at the two antennas are decorrelated, resulting in a decreased correlation coefficient. This leads to a deterioration in measurement accuracy. Thus, the optimal size of the antenna base B at which the error in estimating the ordinates of the LA relief is minimal is 70–80 cm.

For the given irradiation geometry, the size of the antenna base strongly depends on the characteristics of small roughness σ_χ on the surface of a larger LA relief, which also leads to noticeable correlation of the reflected signals received by the antennas. As a result of irradiation of the surface of the LA, we obtain the radio-brightness pattern of reflection of the resolution elements, on which the phase-difference dependence is superposed, covering all the resolution elements of the LA. This is the source material for constructing the relief of the LA.

4. NUMERICAL REALIZATION OF THE ALGORITHM FOR ESTIMATING DANGEROUS IRREGULARITIES AND FOREIGN OBJECTS ON A HELICOPTER LANDING AREA

The proposed algorithm for visualzing and estimating dangerous irregularities and foreign objects on a helicopter landing area using the intensity of radar signals scattered by the surface from different angles of observation and radar interferometric survey results were checked by computer simulation in the OCTAVE software package. To model the surface of the LA and form the radar relief, a phenomenological model [15]. According to this model, the reflecting surface shown in Fig. 5 is modeled as a set of independent elementary reflectors, "shiny points" located at some distance of the surface correlation interval l_z. The ordinates of reflectors of small surface irregularities $\chi(x, y)$ are distributed according to a normal law. For this approach, the signal reflected from each resolution element is the sum of the partial signals from reflectors within this element.

$$\dot{U}_{\Delta S}(t) = \sum_{i=0}^{n_x-1}\sum_{j=0}^{n_y-1} U_{i,j\Delta S}(t), \quad (8)$$

where n_x and n_y are the numbers of partial reflectors along the x and y axes, respectively.

In Fig. 5, the reflectors participating in this simulation cycle are shown in darker color. To form the radar terrain, the following parameters were chosen: length of the linear antenna $l_a = 0.8$ m, the antenna base of the interferometric survey $B = 0.7$ m and helicopter flight altitude $H = 75$ m, the range of angles of sight from the vertical $\theta = 30°$–60°, surface correlation interval $l = 0.2$ m. Number of reflectors n_x and n_y involved in the formation of the echo signal from each element of resolution were determined by the x and y axes as $n_x = \Delta x/l$, $n_y = \Delta x/l$ respectively.

After the phase-difference image was obtained, an operation was carried out to eliminate the Earth's flat surface component. To solve the phase deconvolution problem, one of the basic two-dimensional phase

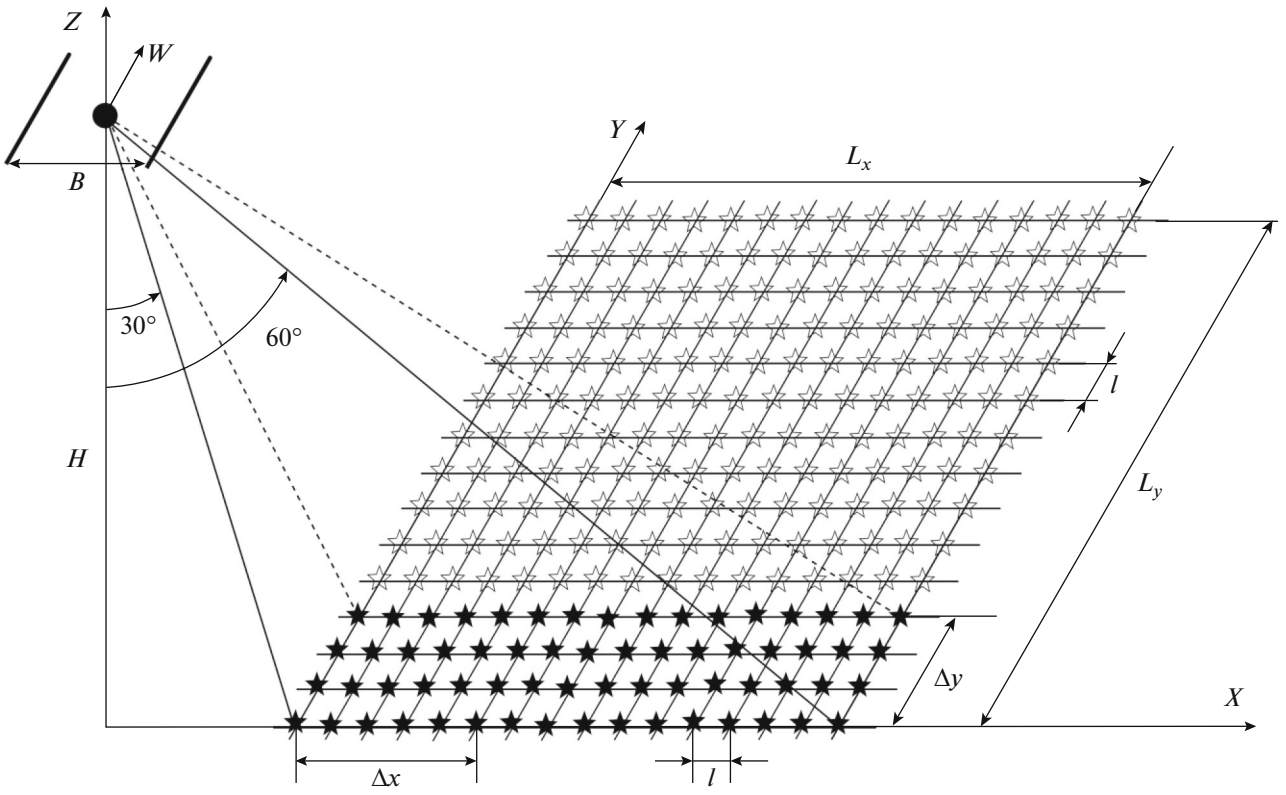

Fig. 5. Diagram of reflectors on LA.

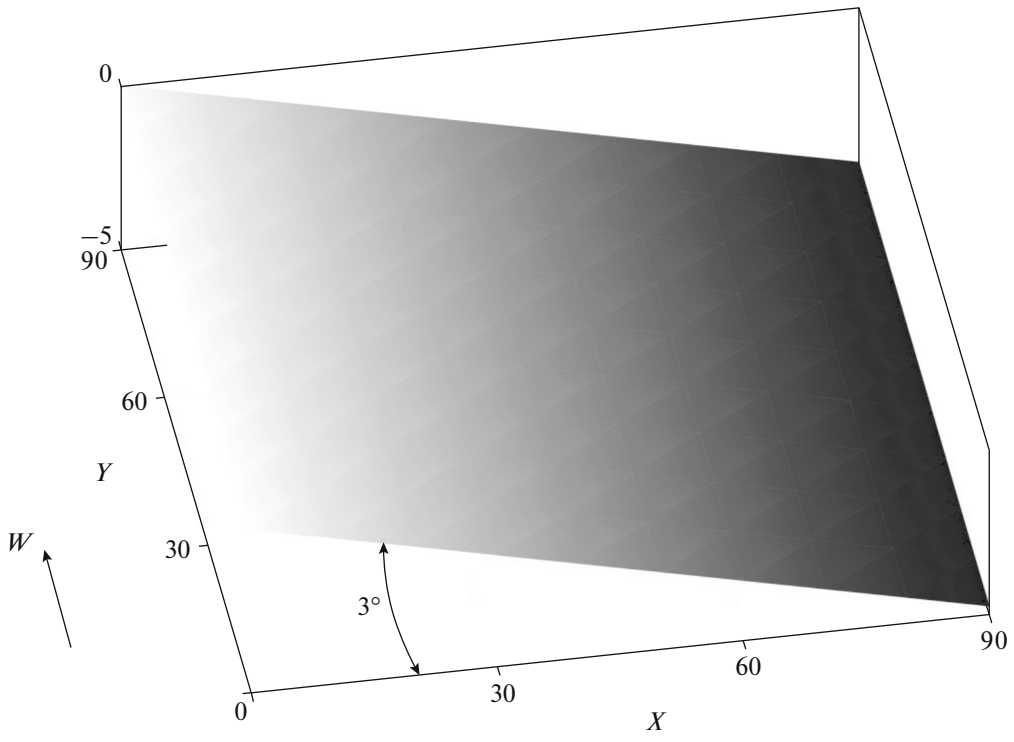

Fig. 6. Surface of large relief with slope of 3°.

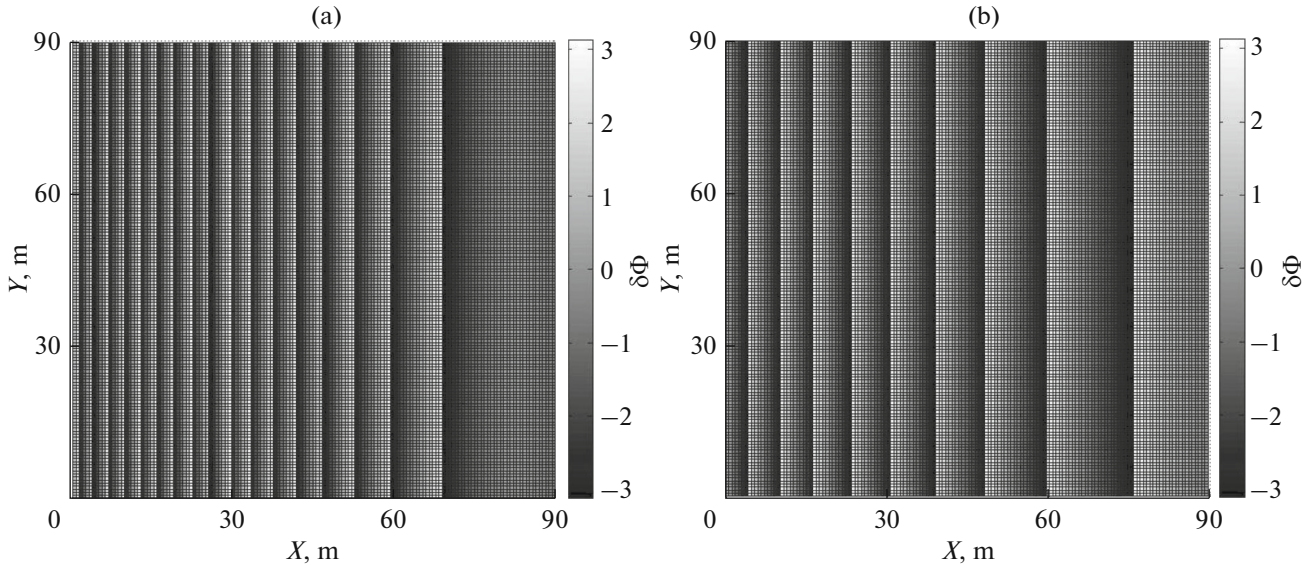

Fig. 7. Interferogram of surface of large relief with slope of 3° (a) and final interferogram (b) obtained after elimination of Earth's flat surface component, background/noise ratio = 20 dB.

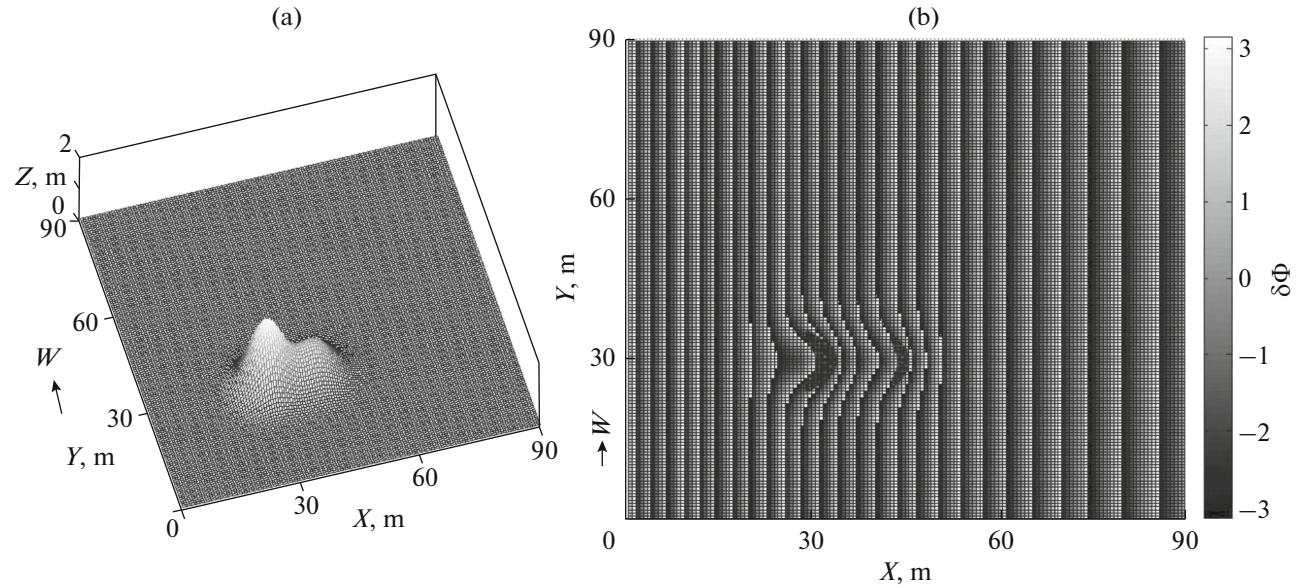

Fig. 8. Plowed field with double-topped hill (a), corresponding interferogram (b), background/noise ratio = 20 dB.

deconvolution algorithms, the least squares method, was chosen [19]. It is easy to show that the dependence between the phase-difference values in each resolution element and changes in the height of the relief is determined by the expression

$$z = \frac{\lambda H \tan\theta}{4\pi B \cos\theta}\delta\Phi' = k_2\delta\Phi', \qquad (9)$$

where $\delta\Phi'$ is the deconvoluted phase. Then, from (9) it follows that in order to obtain data on the ordinates of the relief, the reconstructed phase values should be multiplied by the scaling factor of the deconvoluted phase, depending on the wavelength, base size, helicopter flight altitude, and the elevation angle of the target.

Let us consider the simulation results of interferometric signal processing, obtained by irradiating the surface of the LA in the form of a plowed field with a slope of 3° (Fig. 6). The rms ordinate of roughness for the plowed field and its irregularities is 7.8 mm, and the dielectric constant is $5.9 + j3.5$. Figure 7 shows the obtained interferograms before and after elimination of the Earth's flat surface component.

Figure 8a shows the LA model in the form of a plowed field with a double-topped hill, the maximum height of which is 2 m; Fig. 8b, the phase-difference

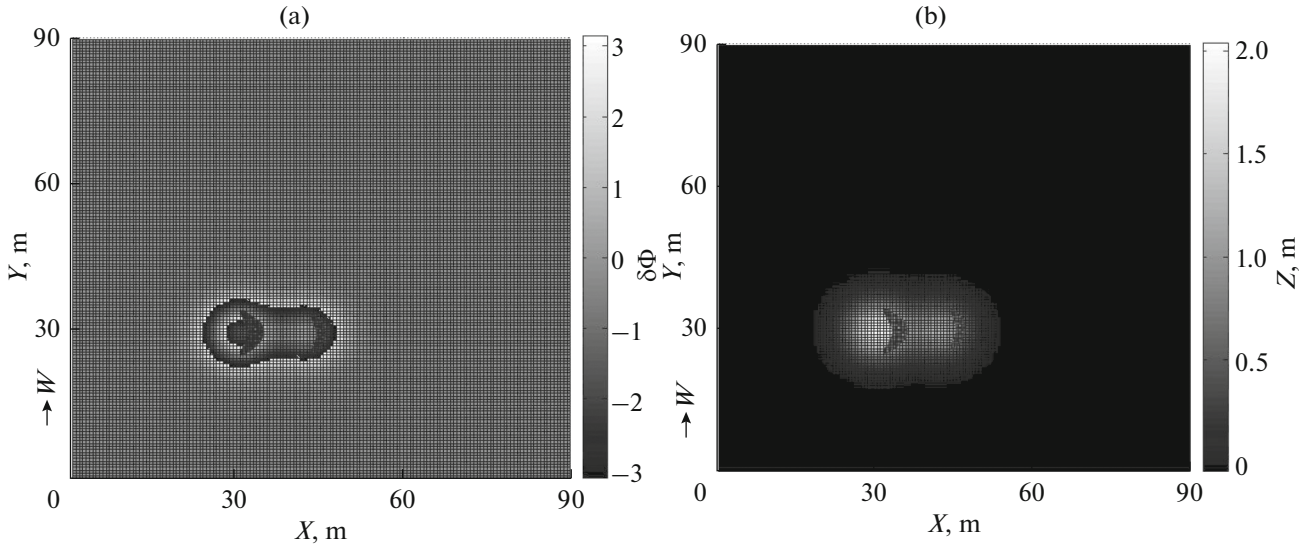

Fig. 9. Interferogram obtained after elimination of flat surface component (a) and reconstructed relief (b), background/noise ratio = 20 dB.

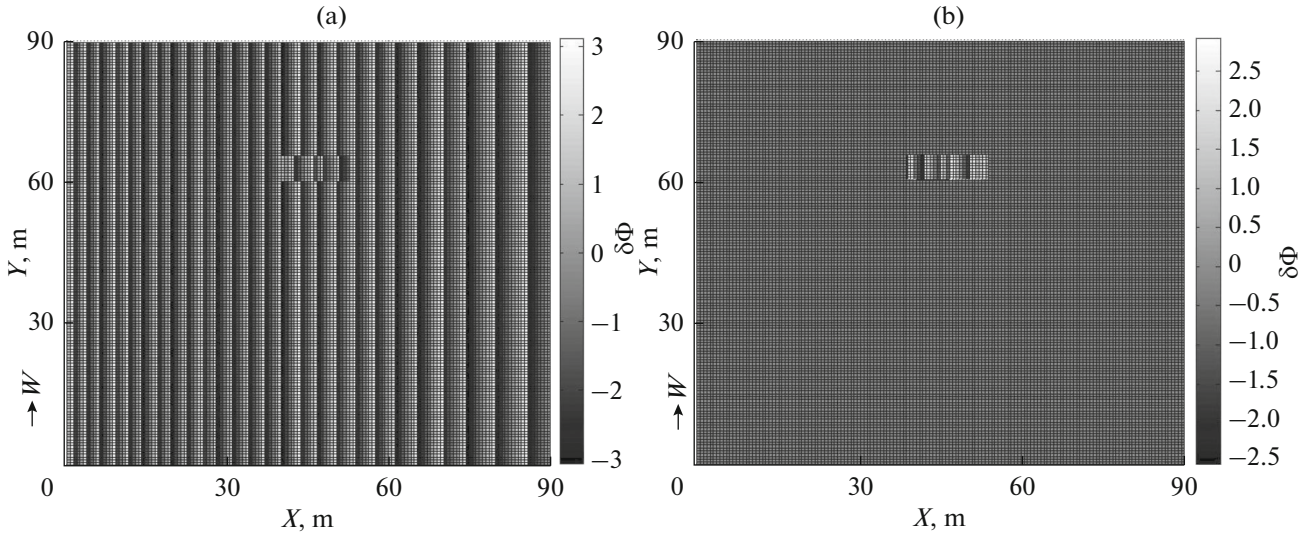

Fig. 10. Interferogram corresponding to presence of car on asphalt road (a) and interferogram obtained after elimination of flat surface component (b), background/noise ratio = 20 dB, signal/(background + noise) ratio = 5 dB.

interferogram of the surface. The results of reconstructing the relief after elimination of the flat surface component are shown in Fig. 9. The error in determining the height of the hill from the interferogram was 3.5 cm.

Figure 10 shows the results of simulatiing an asphalt surface with a car located on it. Clearly, when phase-difference information of the reflected signals arriving at the two antennas is used, visualization of man-made objects on the LA increases significantly. The rms ordinate of roughness of the asphalt surface is 1.5 mm, and the dielectric constant is $2.5 + j0.65$.

CONCLUSIONS

The paper analyzes an algorithm for onboard radar interferometric survey of the surface of an LA. It is shown that the results of the interferometric survey using a linear three-scale model of a reflecting surface makes it possible with the required accuracy to reconstruct a high-quality three-dimensional image of the LA with determination of the nature of the relief.

The initial material for constructing the LA relief is the brightness pattern of reflection by resolution elements obtained after irradiation of the LA surface; the

phase-difference dependence is superposed on this, covering all resolution elements of the LA. These transformations significantly increase the visualization of man-made objects on the LA. The most significant impact on the accuracy in measuring the roughness of irregularities comes from the error in measuring the phase difference of the interferometer signals. At the same time, the detection reliability increases with an increase in the measurement ratio.

FUNDING

This work was supported by the Russian Science Foundation (project no. 14-49-00079) and the Russian Foundation for Basic Research (project no. 18-37-00184).

REFERENCES

1. O. V. Bolkhovskaya, A. A. Mal'tsev, and K. V. Rodyushkin, Izv. Vyssh. Uchebn. Zaved. Radiofiz. **48**, 446 (2005).
2. V. T. Ermolaev, Izv. Vyssh. Uchebn. Zaved. Radiofiz. **38**, 841 (1995).
3. G. S. Kondratenkov and A. Yu. Frolov, *Radio-Wave Imaging. Radar Systems for Remote Sensing of the Earth* (Radiotekhnika, Moscow, 2005) [in Russian].
4. B. Kutuza, M. Bondarenko, D. Dzenkevich, et al., in *Proc. 6th Eur. Conf. on Synthetic Aperture Radar (EUSAR-2006), Dresden, May 16–18, 2006* (EUSAR-2006), p. 637.
5. *Guide to Flight Operation of the Mi-8 Helicopte*r (Avia-Media, Moscow, 2005) [in Russian].
6. A. Nashashibi, T. Fawwz, F. T. Ulaby, and K. Sarabandi, IEEE Trans. Geosci. Remote Sens. **34**, 561 (1996).
7. Sein Khtu and A. I. Baskakov, Radiotekh. i Telekom. Sist., No. 2, 49 (2011).
8. A. J. Gatesman, T. M. Goyette, J. C. Dickinson, et al., Proc. SPIE **4370**, 440070 (2001).
9. Li E. Shih-Syou, Millimeter Wave Polarimetric Radar System as an Advanced Vehicle Control and Warning Sensor. A Doctoral Dissertation for a Degree of Doctor of Philosophy (Electrical Engineering). Ann Arbor: Univ. of Michigan, 1998. 220 p. http://www.eecs.umich.edu/radlab/html/techreports/RL965.pdf.
10. R. P. Bystrov, A. V. Sadykov, and R. N. Chekanov, Radiotekhnika, No. 1, 19 (2005).
11. V. S. Verba, Radiotekhnika, No. 9, 32 (2004).
12. A. B. Borzov, A. V. Sokolov, and V. E. Suchkov, Zarubezh. Radioelektron., No. 5, 55 (2001).
13. A. B. Borzov, R. P. Bystrov, A. V. Petrov, et al., Elektromagn. Volny i Elektron. Sist., No. 6, 17 (2000).
14. N. S. Akinshin, R. P. Bystrov, A. V. Petrov, and R. R. Sadykov, Nauchn. Vestn. MGTU GA, Ser. Radiofiz. i Radiotekh., No. 24, 94 (2000).
15. A. I. Baskakov, T. S. Zhutyaeva, and Yu. I. Lukashenko, *Locational Methods of the Research of Objects and Environments* (Akademiya, Moscow, 2011) [in Russian].
16. A. I. Baskakov and Ka Min Kho, Issled. Zemli iz Kosm., No. 2, 43 (1998).
17. Sein Khtu and A. I. Baskakov, Vestn. MEI, No. 6, 213 (2013).
18. Sein Khtu and A. I. Baskakov, Elektron. Zh. Trudy MAI, No. 57 (2012). http://www.mai.ru/science/trudy/published.php?ID=30698.
19. D. C. Ghiglia and L. A. Romero, J. Opt. Soc. Am. **11** (1), 107 (1994).